**Effect of femoral head size, subject weight and activity level on acetabular cement mantle stress following total hip arthroplasty.**

J.F. Del-Valle-Mojica[1], M.T. Alonso-Rasgado[2], D. Jimenez-Cruz[1], C.G. Bailey[2], T.N. Board[3]

[1]*The University of Manchester, Manchester, United Kingdom.*
[2]*School of Engineering and Materials Science, Queen Mary University of London, London, United Kingdom*
[3]*Wrightington Hospital, Wigan and Leigh NHS Foundation Trust, Lancashire, United Kingdom.*

Author Contributions Statement:
"All authors have contributed to drafting and critically revising the manuscript for important intellectual content. All authors have approved the final submitted manuscript."

Corresponding Author:

Professor M.T. Alonso-Rasgado[2]
Professor of Mechanical Engineering
School of Engineering and Materials Science
Queen Mary University of London
London E1 4NS
UK
email: t.alonso@qmul.ac.uk

**Abstract**

In cases where cemented components are used in total hip arthroplasty, damage or disruption of the cement mantle can lead to aseptic loosening and joint failure.

Currently, the relationship between subject activity level, obesity and prosthetic femoral head size and the risk of aseptic loosening of the acetabular component in cemented THA is not well understood. This study aims to provide an insight into this. Finite element models, validated with experimental data, were developed to investigate stresses in the acetabular cement mantle and pelvic bone resulting from the use of three prosthetic femoral head sizes, during a variety of daily activities and one high impact activity (stumbling) for a range of subject body weights.

We found that stresses in the superior quadrants of the cortical bone-cement interface increased with prosthetic head size, patient weight and activity level. In stumbling, average von Mises stresses (22.4MPa) exceeded the bone cement yield strength for an obese subject (143kg) indicating that the cement mantle would fail.

Our results support the view that obesity and activity level are potential risk factors for aseptic loosening of the acetabular component and provide insight into the increased risk of joint failure associated with larger prosthetic femoral heads.

Words: 199

Keywords: finite element; total hip arthroplasty; femoral head; cement mantle, cemented acetabular cup

## Introduction

Over the past decade, larger femoral heads have gained popularity in Total Hip Arthroplasty (THA) [1, 2, 3]. Reduction of dislocation occurrences and improvement of joint stability has been a key factor in surgeons increasingly favouring larger head sizes [1, 4, 5]. Although improvements in joint stability have been obtained with larger heads, recent data from several sources indicates that they are associated with higher failure rates [2, 6].

Aseptic loosening continues to be one of the most common reasons for revision of hip arthroplasties [2, 7, 8]. Risk factors for aseptic loosening following THA include patient, component and surgical technique factors [8]. Two potential patient factors which have been identified are activity level and obesity [8] however, research to date has not firmly established a relationship between these factors and the risk of aseptic loosening. Flugsrud et al [9] found that patients with upper-quartile body weight were at increased risk of revision for aseptic loosening of the femoral component. More recently, Electricwala et al [10] reported that obesity was associated with early total hip revision due to aseptic loosening, however another study the same year found that BMI was not a risk factor for mechanical failure or aseptic loosening [11]. There is some evidence to suggest that physical activity level is linked to risk of aseptic loosening [9, 12]. Flugsrud et al [9] determined an increased risk of revision for loosening of the acetabular cup in male subjects with higher leisure activity levels and Lübbuke et al. [12] found that the revision risk for femoral component loosening in patients increased significantly with increasing levels of activity.

In cases where cemented components are used in THA, failure or fracture of the cement mantle can lead to aseptic loosening of the acetabular or femoral components, therefore the

long term stability of the joint is dependent upon the cement mantle remaining mechanically sound [13]. For cemented acetabular components the area of greater stresses is located in Zone 1 of the Charnley-DeLee system where failure of the bone-cement interface manifests as demarcations [14, 15, 16]. The demarcations are detected during X-ray inspections as radiolucent lines and are considered a prelude to implant failure [14, 17]. The service life of the cemented components is adversely affected by increases in stress in the cement mantle resulting in a corresponding reduction in fatigue life [18].

To date only limited research has been undertaken into determining the effect of femoral head size on the cement mantle stresses. Lamvohee *et al* [19], using finite element modelling, investigated the stresses in the acetabular cement mantle resulting from the use of two femoral head sizes (22 mm and 28 mm). They found that under the loading condition of normal walking the tensile stresses in the cement mantle increased by up 27% when femoral head size increased from 22 mm to 28 mm. Other studies have also investigated the use different femoral head sizes, however the research was primarily focused on aspects of joint stability rather considering stresses within the joint [20, 21].

A number of studies have investigated acetabular cement mantle stresses but limited their investigations to a single loading condition, that corresponding to normal walking [14, 18, 19, 22, 23, 24]. Tong *et al* [18] analysed acetabular cement mantle stresses under the loading conditions corresponding to normal walking, walking up stairs and walking down stairs using finite element modelling. Tong found higher stresses occurred in the posterosuperior quadrant of the joint with walking downstairs being the most severe activity producing a maximum von Mises stress of 5.4 MPa at the bone-cement interface; however, the study considered only one femoral head size of 22.2 mm and it was conducted using bovine hip

geometry. Wang *et al* [25] subjected bovine hip samples implanted with cemented cups to fatigue loading until failure replicating the loading of normal walking, ascending stairs, descending stairs and single leg stance and found that failure occurred at the bone-cement interface in all cases; however, the study also considered just one femoral head size, 22 mm. Zhang *et al* [42] developed a pelvic bone model which they validated with data from cadaveric experimentation. The authors adapted the model to incorporate simulation of a cemented acetabular cup and investigated the effect on bone-cement interfacial response of non standard cup orientation, non uniform cement thickness and subject-specific versus homogenous trabecular bone material properties for normal walking and stair descending activities. They found that for the single head and cup size considered, both non standard cup orientation and non uniform cement thickness elevated peak stress near the bone-cement interface and that the homogenous model underestimated peak bone-cement interface stress compared to the subject specific model. Sanjay *et al* [43] developed a 3D FE model and used it to investigate the effect of uniform and non-uniform cement mantle thickness on the strain energy density (SED) and tensile stress distribution in the cement mantle of a hip during normal walking, They found that a non-uniform cement mantle thickness affected tensile stress in the cement mantle, in particular, stress was found to increase significantly with a decrease in cement mantle thickness in the superior direction. Zant *et al* [45] describe the use of a new hip simulator to undertake an in vitro study of fatigue behaviour in prosthetic acetabula cemented in bovine pelvic bone backed by FE analysis. Loading corresponding to normal walking and descending stairs for body weights of 75-125 kg was considered. A single femoral head size and a uniform cement mantle (3.5mm) were employed. The study found that debonding at the bone-cement interface in the posterior-superior quadrant, the region where greatest stress occurred, was the main failure mechanism. Lamvohee *et al* [46] describe a FE based investigation into the effect on acetabular bone cement stress of cement

mantle thickness, acetabular size (46, 52 and 58mm diameter) and body mass index (20, 25 and 30 BMI) following total hip arthroplasty considering a 22mm prosthetic femoral head and loading corresponding to the normal walking activity. The authors report an increase in acetuabular size or cement mantle thickness results in a reduction in peak cement mantle stresses and an increase in the number of cycles to failure, whereas an increase in BMI generates increased stresses in the cement mantle resulting in a corresponding reduction in the number of cycles to failure.

This paper describes an investigation into the stresses in the acetabular cement mantle and pelvic bone resulting from the use of prosthetic femoral head sizes of 28 mm,32 mm, and 36 mm, in subjects of different body weights during a range of daily activities: one leg stand, normal walking, ascending stairs, descending stairs in addition to a critical high impact activity, stumbling. The present study is an extension of our previously published work [28]; here we investigate different (loading) activities and body weight (obesity).

**Materials and methods**

A total of 75 scenarios were considered these encompassed 3 femoral head sizes (28 mm, 32 mm and 36 mm) and the 4 daily activities plus 1 critical high load activity for subjects of average height of 1.78 m and a range of body weights: average weight (82 Kg, BMI; 25.8,), overweight (95 Kg, BMI 29.9), obese I (111 Kg, BMI 34.9), obese II (127 Kg, BMI; 39.9) and obese III (143 Kg; BMI; 44.9) [26, 27] (Figure 1)

These scenarios were simulated using Finite Element (FE) models created from CT scan data to simulate artificial hip joints with cemented all-polyethylene acetabular cups. The models were validated with experimental work using an artificial composite Sawbones® hemipelvis

implanted with all-polyethylene cemented acetabular cup with an outer and inner diameter of 50 mm and 36.5 mm respectively. Surface strains obtained using Digital Image Correlation (DIC) were compared against predictions from the 36 mm head FE model run under the same loading conditions [28]. DIC has been demonstrated to be a valid and accurate technique for surface strain measurement in biomechanics, in particular for pelvic constructs [44].

The stress analysis was carried out at three main regions of interest identified as A1, A2 and A3 (Figures 2a, 2b, 2c). Region A1 and A2, located within the boundaries where the major load transfer occurs [22], correspond to the superior and anterior periacetabular bone areas, respectively. Region A3 corresponds to the cement mantle interfaces "bone-cement" and "cement-cup" responsible for fixing the implant to the pelvis and where the load transfer between bone and implant occurs [29, 30]; failure of the "bone-cement" interface may lead to aseptic loosening, cup migration and final gross failure [22].

**Finite Element Model**

Computer tomography (CT) data of an artificial composite fourth generation Sawbones® (AG, Sweden) hemipelvis, implanted with a cemented all-polyethylene acetabular cup with an outer and inner diameter of 50 mm and 36.5 mm respectively (Figure 3a), was used to construct a total of 75 FE models, to investigate the 3 femoral head sizes (28 mm, 32 mm and 36 mm).

The CT data was imported into the segmentation software Avizo (FEI Visualization Sciences Group, Berlin, Germany) to create segmentation masks of the pelvic bone that included cortical and trabecular sections, and for the non-uniform thickness cement mantle. Each mask was exported as a separate set of CT slices with a thickness of 0.5 mm, transverse resolution

of 400 x 400, and pixel size of 0.5 x 0.5 mm; a total of 485 CT slices for the pelvic bone and 181 for the cement mantle. The two CT slice sets were imported into 3D image segmentation and processing software enabling individual 3D surfaces for the cortical bone, trabecular bone and cement mantle to be generated (Figure 3a).

Each of the 3D surfaces was exported in IGES file format and imported into Abaqus 6.13 (Dassault Systemes, RI, USA) to create the complete model assembly that also included the femoral head and acetabular cup geometries (created in Abaqus 6.13 (Figures 3b,3c)); following the model assembly, the finite element mesh was created in Abaqus 6.13 (Figure 3d). Quadratic tetrahedral elements (C3D10) were used for the pelvic bone and cement mantle, whereas quadratic hexahedral elements (C3D20R) were used for the acetabular cup and femoral head.

*Boundary Conditions*

The sacro-iliac joint and pubis symphysis were fixed: displacements and rotations in all directions were defined as zero [14, 18, 23, 24, 31, 32]. Fully bonded conditions were defined for the bone-cement and cement-cup interfaces [33]. Frictionless tangential behaviour between femoral head and cup was defined with a surface-to-surface contact interaction, which has been shown to be a reasonable assumption [19, 22]. For the contact simulation between the femoral head and acetabular component, a stiffness scale factor of 1 and a penetration tolerance (relative) of 0.001 were employed. The peak reaction force (RF) of each of the investigated activities was applied as a concentrated force at the central node of the femoral head (Figures 4a,4b). The magnitude and angle of the load was modified accordingly for the scenarios simulated [34]; Table 1 summarises the loading angles and peak reaction force magnitudes used in the numerical models for all activities and

subjects investigated.

*Materials*

Linear elastic isotropic behaviour was assumed for all the materials considered in the FE models, including the pelvic bone [41]. The mechanical properties for cortical shell and trabecular core of the pelvic bone were obtained from the manufacturer of the artificial hemipelvis. The model considered cross linked ultra-high molecular weight polyethylene (UHMWPE) for the acetabular cup, poly-methyl-methacrylate (PMMA) bone cement for the cement mantle and steel for the femoral head; with corresponding mechanical properties assigned in accordance with the literature [18, 29, 30, 35]. Table 2 summarises the mechanical properties assigned to each of the different model components.

*Mesh sensitivity*

The accuracy of the FE model predictions was assessed by undertaking a mesh sensitivity analysis that consisted of investigating the effect on pelvic bone and cement stress of varying the mesh density of the model components (hemipelvis, cement mantle, acetabular cup and femoral head) for the three femoral head sizes. The loading condition of the average subject undertaking one leg stand was used for the analysis. A comparison of the predicted pelvic bone and cement mantle stresses produced by three mesh densities (coarse, medium and fine) was undertaken. The medium density mesh was chosen for all the components as only a 1% maximum variation in pelvic bone and cement stresses was found when compared against the fine mesh. Table 3 shows the number of elements employed for the coarse, medium and fine meshes employed in the sensitivity analysis**.**

**Experimental work: Finite element model validation**

The finite element model was validated with data obtained from experimental work undertaken on an artificial composite Sawbones® hemipelvis. CT scan data of the composite hemipelvis was used to create the FE model and surface strain predictions compared with experimentally obtained values considering the same loading conditions. The experimentation consisted of the application of a compressive load of 1800 N, equal to the peak reaction force at the hip joint during one leg stand activity for a subject of body weight 70 Kg [34], after which surface strains were obtained using Digital Image Correlation (DIC) at three regions on the hemipelvis, A1-1 (300 $mm^2$), A1-2 (250 $mm^2$) and A2 (1600 $mm^2$), defined as shown in Figure 2. A 36 mm steel ball bearing was used to simulate the femoral head, this was inserted into the acetabular cup and used to apply the compressive loading. Repeatable DIC measurements were ensured by the application of 10 loading cycles, with load ranging from 1200 N to 1800 N in increments of 200 N from which the coefficient of variation (CV) for the measurements was calculated. The experimental measurements were compared against the predictions of the FE model for the 36 mm femoral head obtained under the same loading conditions as the experimentation.

*Experimental setup*

Compressive loading was applied using a single column universal testing machine (Instron 3342, Instron, MA, USA) using a 2 KN load cell to which the 36 mm steel ball bearing was attached with a custom-made steel taper (Figure 5). A holding device was used to fix the pelvis by clamping the sacro-iliac joint and supporting the pubis symphysis (Figure 5). The DIC system used for the deformation measurements and vertical surface strain measurements consisted of an array of two 5-megapixel cameras with focal length of 12 mm, a computer interface plus data acquisition and processing software (Figure 5).

*Experimental procedure*

A speckle pattern, used by the DIC system to track the deformation of the pelvis and calculate the surface strains, was created over the hemipelvis using black paint sprayed sparsely over an initial layer of white paint. The painted hemipelvis was then secured in the universal testing machine using the holding device so a loading angle of 6.5º with the vertical axis was achieved [34].

Calibration of the DIC system was undertaken following the guidelines of the manufacturer prior to the measurements [36]. When recording the image data at regions A1-1 and A1-2 the cameras were set at a distance of 280 mm from the hemipelvis. Loading ranging from 1200 N to 1800 N was applied in increments of 200 N; the loading cycle was repeated 10 times.

First, an image of the hemipelvis in its initial state (unloaded/non-deformed) was recorded before each load was applied. A displacement control of 1 mm/min was set for the application of all loads. Once the set load was reached, a three minute period was observed to allow the system to stabilise, after which the image of the final state (loaded/deformed) of the hemipelvis was recorded. After completion of A1-1 and A1-2 measurements, the cameras were moved and set for measurements at region A2 following the same procedure.

*Data Processing*

After completion of all measurements for regions A1-1, A1-2 and A2, image data obtained for the hemipelvis at initial and final states for each load was processed in Aramis V6.1. Vertical surface strains were computed using a strain computation mask created over the surface of the composite hemipelvis; the mask consisted of quadrangular facets of 20 pixels

by 20 pixels with a 10 pixels step between facets. A linear strain computation algorithm in Aramis V6.1 was used to calculate the vertical surface strains.

To eliminate potential measurement noise an average noise filter was applied to all the post-processed data. The statistics tool within Aramis V6.1 was used to calculate the average vertical surface strain within regions A1-1, A1-2 and A-2 for each of the ten measurements for all load cases (1200 N, 1400 N, 1600 N, 1800 N); the individual values were recorded and the average of 10 measurements for each load was calculated and used to compare against the predictions of the FE model.

In order to assess the repeatability of the experimental measurements at regions A1-1, A1-2 and A-2, the mean and standard deviation (Std. Dev.) of the surface strain measurements were calculated for each region and load from which the coefficient of variation (CV) was calculated. The maximum CV for the regions was 5%.

Following validation of the 36 mm head model, the femoral head and acetabular cup dimensions were modified accordingly to construct the 28 mm and 32 mm head models (Table 4). An investigation into the pelvic bone (A1, A2) and cement mantle stresses (A3) was then undertaken for the three femoral head sizes (28 mm, 32 mm, 36 mm) for average weight, overweight, obese I, obese II and obese III subjects [21, 22] undertaking daily activities of one leg stand, normal walking, ascending stairs and descending stairs, and also the critical high load activity, stumbling.

## Results

In Figures 6-10 average von Mises stresses for cortical and trabecular bone are presented at the superior region A1 and anterior region A2. The stresses in the cement mantle are presented for individual quadrants of the bone-cement and cement-cup interfaces. All the quadrants are of equal area of 1,120 $mm^2$ and identified as follows: (1) anterosuperior, (2) posterosuperior, (3) anteroinferior and (4) posteroinferior.

### FE Model validation: Vertical surface strains in regions A1 (A1-1, A1-2) and A2:

Vertical surface strain predictions for pelvic bone regions A1 (A1-2, A1-2) and A2 obtained from the 36 mm head FE model compared well with experimentally obtained values; differences of 1 - 5% were determined for the load cases considered, 1200-1800 N [28]. In the superior periacetabular region, average surface strain values of 112-168με were recorded experimentally for location A1-1; corresponding FE model predictions were 117-175με. For A1-2, experimental values were in the range 236-364με with FE predictions 240-360με. FE model predictions of between 100-151με were obtained for the anterior periacetabular region (A2), compared to 104-158με from the experimentation.

### Daily activities: one leg stand, normal walking, ascending stairs, descending stairs for the average weight (82 kg), overweight (95 kg), obese I (111 kg), obese II (127 kg) and obese III (143 kg) subjects considering the three femoral head sizes (28 mm, 32 mm and 36 mm).

*Periacetabular Bone*

Figure 6 shows a comparison of the predicted average von Mises stress in the periacetabular bone in the superior (A1) and anterior (A2) regions. The trabecular bone stresses remained invariant across all activities and femoral head sizes. For all subjects average von Mises stress in the superior periacetabular region were 0.9-1.5 MPa (41-56%) higher in cortical bone and 0.2 MPa (33-100%) higher in trabecular bone than corresponding values in the anterior periacetabular region. In addition, stresses in cortical bone were 6-12 times greater than those in the trabecular bone. Whilst average von Mises stress in trabecular bone did not vary with activity, stresses in cortical bone generated by the descending stairs activity were 6-14% higher than those for the one leg stand. Stresses in both cortical and trabecular bone remained invariant with femoral head size across all activities. Body weight affected stresses in both cortical and trabecular bone with stress increasing with greater body weight. Stresses in the cortical bone of the obese III subject were 1.6-2.1 MPa (59-76%) higher than corresponding values for the average weight subject. For trabecular bone, values were 0.4 MPa higher in all cases.

*Cement interfaces: bone-cement and cup-cement*

A comparison of the average von Mises stress in the superior quadrants of the bone-cement and cement-cup interfaces is shown in Figure 7, the same comparison for the inferior quadrants is shown in Figure 8. Within the superior quadrants (Figure 7), higher average von Mises stresses (10-40%) occurred at the cortical bone-cement interface compared to the trabecular bone-cement interface for the three femoral head sizes and across all the activities investigated. Stresses in the cement-cup interface were generally greater than those at the trabecular bone-cement interface but less than those of the cortical bone-cement interface. Across all activities, the one leg stand resulted in the lowest stresses generated (2.0-4.8MPa);

this was the case for cortical bone-cement, trabecular bone-cement and cement-cup interfaces and for the three femoral head sizes considered. The highest stresses (2.3 - 5.1MPa) resulted from descending stairs.

Stresses increased with subject weight. In the obese III subject, stresses were greater than corresponding values for the average weight subject by between 50 and 100%. In general, average von Mises stress increased with femoral head size, with stresses for the 36mm head case 0.1-0.2 MPa greater than corresponding values for the 28mm head.

Stress levels within the inferior quadrants (Figure 8) were lower than those in the superior quadrants. In addition, average von Mises stresses in the anteroinferior and posteroinferior quadrants of the trabecular bone – cement interface and the posteroinferior quadrant of the cement – cup interface didn't vary with activity or femoral head size. The ascending and descending stairs activities resulted in stress levels that were 0.1MPa higher than for one leg stand and normal walking, and, for a given activity, stresses also increased by 0.1MPa with increasing head size.

**Critical high impact activity: stumbling, for average weight (82 Kg), overweight (95 Kg), obese I (111 Kg), obese II (127 Kg) and obese III (143 Kg) subjects.**

*Periacetabular bone*

Figure 9 shows a comparison of the predicted average von Mises stress in the periacetabular bone in the superior (A1) and anterior (A2) regions. It can be seen upon inspection of this figure that, the greater average von Mises stresses were experienced in the cortical bone of the superior periacetabular region (14.2-24.7MPa). For all bone types and regions, stresses increased with subject weight, increasing by between 63% and 82% between the average

weight and obese III subjects. Stresses did not vary with femoral head size. Comparing the results from Figure 9 to those for the daily activities in Figure 6, it can be seen that the stumbling activity resulted in stresses that were at least three times greater than those generated by the daily activities considered.

*Cement interfaces bone-cement and cup-cement*

A comparison of the average von Mises stress at bone-cement and cement-cup interfaces for stumbling at the superior and inferior quadrants of the bone-cement and cement-cup interfaces is shown in Figure 10. The greatest von Mises stresses occurred in the cortical bone-cement interface in the superior quadrants (12.3-22.4 MPa). In the superior quadrants, stresses increased with subject weight, increasing by between 62% and 74% between the average weight and obese III subjects. Average von Mises stress increased slightly with femoral head size (1-2% in cortical bone between 28 and 32mm femoral head sizes). Bone cement stresses resulting from stumbling (Figure 10) were more than three times higher than corresponding stresses resulting from the daily activities (Figure 7).

Stresses in the inferior quadrants were lower than in the superior quadrant. In the trabecular bone-cement interface of the inferior quadrants stresses ranged from 2.6-5.6MPa; in the cement-cup interface the range was 3.2-6.6MPa. Stresses increased with subject weight, increasing by between 65% and 77% between the average weight and obese III subjects.

**Discussion**

It has been reported that rates of aseptic loosening of the acetabular component in cemented THA are some 2-4 times higher than those of the femoral component [22]. Aseptic loosening

of the acetabular component is multifactorial with both mechanical and biological components implicated [14, 22]. Mechanically, high stress in the cement or mantle pelvic bone may be a contributing factor. High stress in the bone cement mantle can lead to damage, crack initiation and propagation, exposing the bone-cement interface to wear debris leading to debonding and eventually, to failure of the joint [14,22].

The results from our study indicate that in general the load across the pelvic bone is supported predominantly by the cortical bone and that the majority of the load is transferred to the pelvis through the superior region of the acetabular rim where we found average von Mises stresses were the highest, a finding supported elsewhere in the literature [37]. We found that whilst pelvic bone stresses remained invariant to the size of the prosthetic head employed for all the scenarios considered, the stresses were affected by daily activity and patient body weight. Cortical bone stress increased with body weight. For the obese III subject cortical bone stress was between 58% and 76% higher than corresponding values for the average weight subject for the daily activities. Descending stairs activity generated the highest periacetabular bone stress, 7% to 14% higher than for the one leg stand for the body weights considered. Stresses remained well below the yield stress for all cases suggesting no contribution to aseptic loseining though this pathway for the conditions considered.

As a consequence of the majority of the load beingtransferred to the pelvis through the superior region of the acetabular rim, the highest stresses in the cement mantle in our models occurred at the cortical bone-cement interface in the superior quadrants of the joint (Zone 1 of the Charnley-DeLee system) which is in agreement with previous research [14, 18, 22]. This region is where radiolucent lines are reported to most commonly be observed during X-ray examinations and are associated with an increase in aseptic loosening [16, 17]. In the

cement mantle, stresses were affected by daily activitiy, femoral head size and body weight. Descending stairs resulted in higher cement mantle stress than the other daily activities. The highest von Mises stress in the cement mantle for descending stairs from our study was 5.1 MPa, which compares well with the values reported by Tong et al [18], 5.4 MPa, and Zant et al [45], 4.5 MPa, for the same activity.

Average von Mises stress in the cement mantle varied with femoral head size, being up to 10% greater for the 36mm head than for the 28mm head for the daily activities. This is because for a given acetabular cup size, consideration of a larger femoral head results in a reduction in the acetabular cup thickness. A thinner acetabular cup is less able to help distribute the stresses in the acetabular component itself, consequently more of the compressive loading is transferred directly to the cement mantle [22]. In the obese III subject, stresses were greater than corresponding values for the average weight subject by between 52 and 100% for the daily activities considered. The maximum average von Mises cement stress predicted by the models for the daily activities (5.1 MPa) is below the reported yield strength of the bone cement [38], 21.7 MPa, and also below the bone cement endurance limit, 8.0 MPa, determined by Lewis *et al* [39].

In the high impact activity of stumbling, loads of up to nine times body weight are generated [40]. Our study found that stress in the periacetabular bone and superior quadrants of the cortical bone-cement interface were at least three times greater in stumbling compared to the range of daily activities considered for all femoral head sizes considered. The maximum average von Mises stresses in the anterosuperior quadrant of the cortical bone-cement interface, 22.0-22.4 MPa, exceeded the bone cement yield strength, 21.7 MPa [40], and was almost three times above the bone cement fatigue endurance limit [39], for the obese III

subject for all prosthetic femoral head sizes considered. This suggests that under these circumstances the cement mantle would fail.

Our FE model is subject to assumptions and limitations typically associated with complex numerical simulations of this type. For example, linear elastic isotropic behaviour was assumed for all the materials considered in the FE models, including the pelvic bone. Dalstra *et al* [41] examined the material properties of pelvic bone and determined that it is not highly anisotropic, therefore considering bone to be isotropic is a reasonable modelling assumption which should not introduce significant errors. As a consequence, this common approach has also been employed by a number of researchers previously [18, 19, 22, 23, 24, 32, 37]. Although muscle forces were not explicitly considered, the loads applied to simulate the various activities considered were derived from those reported by Bergmann *et al* [34] using instrumented implants in living subjects which take into account muscle forces. Additional limitations include the fact that static as opposed to cycling loading was considered. Also, the model did not account for bone morphological changes resulting from the consideration of differing body weights. However, the exact relationship between obesity and bone structural and material properties is complex and still being debated with a recent review of available research revealing contrasting findings [46]. A number of studies have indicated obesity plays a protective role in bone health, however recent evidence has indicated that it is a risk factor for decreased bone density and fracture [46]. Based on their review of the existing data available, Palermo *et al* [46] suggest that the relationship between BMI and bone health is U-shaped, with an increase in BMI above eutrophic ranges being (weakly) beneficial for bone health but that this effect disappears for BMIs representative of morbid obesity. They note that more studies are required before a definitive conclusion can be drawn. Furthermore, we validated our FE model with data obtained from experimental work

undertaken on an artificial composite Sawbones® hemipelvis. Good agreement was obtained between experimentally determined surface strains and corresponding numerical predictions which provides a degree of confidence in the results from the FE model we developed.

We reported von Mises stresses for cortical and trabecular bone and the cement mantle. While it could be argued that principal stress may be more suitable for evaluating failure of the cement mantle, we decided to report von Mises stress for several reasons. Firstly, a detailed assessment of failure propensity was outside the scope of our study, this will form the basis of a future study to be developed from the current work, the main focus of the current study was to analyse the changes in stress distribution and magnitude resulting from different femoral head sizes, body weights and activity levels. In addition, numerical values of maximum stress may be high at a point due to surface irregularities. These irregularities may be absent in practice, but are hard to avoid in a numerical model due to non-uniform element sizes. Hence, an average stress was reported. In addition, von Mises stress is directly comparable to the tensile strength of a material [47], and bone cement will fail first under tensile stress rather than under compressive stress (48, 49). Therefore, von Mises stress was used to identify areas of high-stress enabling magnitude to be directly compared against a known tensile strength value, thus providing an indication of the potential for failure. Finally, a number of previous studies used von Mises stress to report mechanical stresses in hip constructs including the cement mantle, see for example [22, 37, 42, 45], therefore, adopting a similar metric may help researchers compare our results with the literature.

In summary, ousr study found that stresses in the superior quadrants of the cortical bone-cement interface increased with prosthetic head size, patient weight and activity level. In stumbling, average von Mises stresses exceeded the bone cement yield strength for an obese

subject (Obese III, 143 kg) indicating that the cement mantle would fail. In terms of stress in periacetabular bone and cement mantle interfaces, patient weight has a greater effect than the daily activities undertaken by the subject considered in this study. An increase in body weight resulted in greater load being transferred to the pelvis (through the superior region of the acetabular rim) resulting in higher bone stress. Similarly, activities which generated higher peak hip contact forces resulted in more load transfer to the pelvis leading to higher bone stress. Although stresses in the bone cement were below yield and the endurance limit for the range of daily activities considered, the risk of debonding at the bone–cement interface may increase where defects at the interface exist, particularly when subjects are obese, or where larger femoral head sizes have been employed or higher level activities are undertaken. This debonding may lead to aseptic loosening and ultimately joint failure. Our results support the view that obesity and activity level are potential risk factors for aseptic loosening of the acetabular component and provide insight into the increased risk of joint failure associated with larger prosthetic femoral heads.

**References**

[1] No authors listed. 2014. 12th Annual Report. National Joint Registry of England, Wales and Northern Ireland. Hemel Hempstead, United Kingdom.

[2] No authors listed. 2017. 14th Annual Report. National Joint Registry of England, Wales and Northern Ireland. Hemel Hempstead, United Kingdom.

[3] No authors listed. 2013. 10th Annual Report. National Joint Registry of England, Wales and Northern Ireland. Hemel Hempstead, United Kingdom.

[4] Triclot, P., & Gouin, F. (2011). Update - 'Big-head': The solution to the problem of hip implant dislocation? Orthopaedics & Traumatology: Surgery & Research, 97(4), S42–S48. https://doi.org/10.1016/j.otsr.2011.03.011

[5] Stroh, D. A., Issa, K., Johnson, A. J., Delanois, R. E., & Mont, M. A. (2013). Reduced Dislocation Rates and Excellent Functional Outcomes With Large-Diameter Femoral Heads. The Journal of Arthroplasty, 28(8), 1415–1420. https://doi.org/10.1016/j.arth.2012.11.017

[6] Zijlstra, W. P., De Hartog, B., Van Steenbergen, L. N., Scheurs, B. W., & Nelissen, R. G. H. H. (2017). Effect of femoral head size and surgical approach on risk of revision for dislocation after total hip arthroplasty. Acta Orthopaedica, 88(4), 395–401. https://doi.org/10.1080/17453674.2017.1317515

[7] Ulrich, S. D., Seyler, T. M., Bennett, D., Delanois, R. E., Saleh, K. J., Thongtrangan, I., Mont, M. A. (2007). Total hip arthroplasties: What are the reasons for revision? International Orthopaedics, 32(5), 597–604. https://doi.org/10.1007/s00264-007-0364-3

[8] Desy, Nicholas M., and Matthew P. Abdel. (2017). Aseptic Implant Loosening. In Complications after Primary Total Hip Arthroplasty, pp. 183-194. Springer, Cham.

[9] Flugsrud, G. B., Nordsletten, L., Espehaug, B., Havelin, L. I., & Meyer, H. E. (2007). The effect of middle-age body weight and physical activity on the risk of early revision hip arthroplasty: A cohort study of 1,535 individuals. Acta Orthopaedica, 78(1), 99–107. https://doi.org/10.1080/17453670610013493

[10] Electricwala, A. J., Narkbunnam, R., Huddleston, J. I., III, Maloney, W. J., Goodman, S. B., & Amanatullah, D. F. (2016). Obesity is Associated With Early Total Hip Revision for Aseptic Loosening. The Journal of Arthroplasty, 31(9), 217–220. https://doi.org/10.1016/j.arth.2016.02.073

[11] Wagner, E. R., Kamath, A. F., Fruth, K. M., Harmsen, W. S., & Berry, D. J. (2016). Effect of Body Mass Index on Complications and Reoperations After Total Hip Arthroplasty. The Journal of Bone and Joint Surgery, 98(3), 169–179. https://doi.org/10.2106/jbjs.o.00430

[12] Lübbeke, A., Garavaglia, G., Barea, C., Stern, R., Peter, R., & Hoffmeyer, P. (2011). Influence of patient activity on femoral osteolysis at five and ten years following hybrid total hip replacement. The Journal of Bone and Joint Surgery. British Volume, 93–B(4), 456–463. https://doi.org/10.1302/0301-620x.93b4.25868

[13] Ramos, A., & Simões, J. A. (2009). The influence of cement mantle thickness and stem geometry on fatigue damage in two different cemented hip femoral prostheses. Journal of Biomechanics, 42(15), 2602–2610. https://doi.org/10.1016/j.jbiomech.2009.06.037

[14] Coultrup, O. J., Hunt, C., Wroblewski, B. M., & Taylor, M. (2009). Computational assessment of the effect of polyethylene wear rate, mantle thickness, and porosity on the mechanical failure of the acetabular cement mantle. Journal of Orthopaedic Research, n/a-n/a. https://doi.org/10.1002/jor.21040

[15] Bernoski, F. P., New, A. M. R., Scott, R. A., & Northmore-Ball, M. D. (1998). An in vitro study of a new design of acetabular cement pressurizer. The Journal of Arthroplasty, 13(2), 200–206. https://doi.org/10.1016/s0883-5403(98)90100-0

[16] Mueller, L. A., Nowak, T. E., Mueller, L. P., Schmidt, R., Ehrmann, C., Pitto, R. P., … Eichinger, S. (2007). Acetabular cortical and cancellous bone density and radiolucent lines after cemented total hip arthroplasty: a prospective study using computed tomography and plain radiography. Archives of Orthopaedic and Trauma Surgery, 127(10), 909–917. https://doi.org/10.1007/s00402-007-0304-0

[17] Zicat, B., Engh, C. A., & Gokcen, E. (1995). Patterns of osteolysis around total hip components inserted with and without cement. The Journal of Bone & Joint Surgery, 77(3), 432–439. https://doi.org/10.2106/00004623-199503000-00013

[18] Tong J, Zant NP, Wang JY, Heaton-Adegbile P, Hussell JG. (2008). Fatigue in cemented acetabular replacements. International Journal of Fatigue, 30(8):1366-75.

[19] Lamvohee, J.-M. S., Mootanah, R., Ingle, P., Cheah, K., & Dowell, J. K. (2009). Stresses in cement mantles of hip replacements: effect of femoral implant sizes, body mass index and bone quality. Computer Methods in Biomechanics and Biomedical Engineering, 12(5), 501–510. https://doi.org/10.1080/10255840902718626

[20] Hoeltzel DA, Walt MJ, Kyle RF, Simon FD. (1989). The effects of femoral head size on the deformation of ultrahigh molecular weight polyethylene acetabular cups. Journal of Biomechanics, 22(11):1163-73.

[21] Girard, J. (2015). Femoral head diameter considerations for primary total hip arthroplasty. Orthopaedics & Traumatology: Surgery & Research, 101(1), S25–S29. https://doi.org/10.1016/j.otsr.2014.07.026

[22] Hua, X., Wroblewski, B. M., Jin, Z., & Wang, L. (2012). The effect of cup inclination and wear on the contact mechanics and cement fixation for ultra high molecular weight polyethylene total hip replacements. Medical Engineering & Physics, 34(3), 318–325. https://doi.org/10.1016/j.medengphy.2011.07.026

[23] Hua, X., Li, J., Wang, L., Wilcox, R., Fisher, J., & Jin, Z. (2015). The effect of cup outer sizes on the contact mechanics and cement fixation of cemented total hip replacements. Medical Engineering & Physics, 37(10), 1008–1014. https://doi.org/10.1016/j.medengphy.2015.08.003

[24] Ghosh, R. (2016). Assessment of failure of cemented polyethylene acetabular component due to bone remodeling: A finite element study. Journal of Orthopaedics, 13(3), 140–147. https://doi.org/10.1016/j.jor.2016.03.001

[25] Wang, J.-Y., Heaton-Adegbile, P., New, A., Hussell, J. G., & Tong, J. (2009). Damage evolution in acetabular replacements under long-term physiological loading conditions. Journal of Biomechanics, 42(8), 1061–1068. https://doi.org/10.1016/j.jbiomech.2009.02.023

[26] OECD (2009), Society at a Glance 2009: OECD Social Indicators, OECD Publishing, Paris.

[27] Marques, A., Peralta, M., Naia, A., Loureiro, N., & de Matos, M. G. (2017). Prevalence of adult overweight and obesity in 20 European countries, 2014. European Journal of Public Health, 28(2), 295–300. https://doi.org/10.1093/eurpub/ckx143

[28] Alonso-Rasgado, T., Del-Valle-Mojica, J. F., Jimenez-Cruz, D., Bailey, C. G., & Board, T. N. (2018). Cement interface and bone stress in total hip arthroplasty: Relationship to head size. Journal of Orthopaedic Research®. https://doi.org/10.1002/jor.24052

[29] Dunne N, Clements J, Wang JS. 2014. Acrylic cements for bone fixation in joint replacement. In: Revell P.A. Joint Replacement Technology, 1st ed. Woodhead Publishing; p 212-256.

[30] Kühn K.D. 2005. What is bone cement? In: Breusch, Malchau. The well-cemented total hip arthroplasty, 2005 ed. Berlin Heildelberg: Springer; p 52-59.

[31] Ghosh, R., Gupta, S., Dickinson, A., & Browne, M. (2012). Experimental validation of numerically predicted strain and micromotion in intact and implanted composite hemi-pelvises. Proceedings of the Institution of Mechanical Engineers, Part H: Journal of Engineering in Medicine, 227(2), 162–174. https://doi.org/10.1177/0954411912461238

[32] Ghosh, R., Pal, B., Ghosh, D., & Gupta, S. (2013). Finite element analysis of a hemi-pelvis: the effect of inclusion of cartilage layer on acetabular stresses and strain. Computer Methods in Biomechanics and Biomedical Engineering, 18(7), 697–710. https://doi.org/10.1080/10255842.2013.843674

[33] Alonso-Rasgado, T., Jimenez-Cruz, D., Bailey, C. G., Mandal, P., & Board, T. (2012). Changes in the stress in the femoral head neck junction after osteochondroplasty for hip impingement: A finite element study. Journal of Orthopaedic Research, 30(12), 1999–2006. https://doi.org/10.1002/jor.22164

[34] Bergmann G., Graichen F., Rohlmann A., Bender A., Heinlein B., Duda G.N., … Morlock M.M. (2010). Realistic loads for testing hip implants. Bio-Medical Materials and Engineering, 20(2), 65–75. https://doi.org/10.3233/BME-2010-0616

[35] Kurtz, Steven M. (2009). A primer on UHMWPE. In UHMWPE Biomaterials Handbook (Second Edition), pp. 1-6.

[36] Aramis User Manual, 2009. GOM, Germany.

[37] Dalstra, M., & Huiskes, R. (1995). Load transfer across the pelvic bone. Journal of Biomechanics, 28(6), 715–724. https://doi.org/10.1016/0021-9290(94)00125-n

[38] Saha, S., & Pal, S. (1984). Mechanical properties of bone cement: A review. Journal of Biomedical Materials Research, 18(4), 435–462. https://doi.org/10.1002/jbm.820180411

[39] Lewis, G., & Ed Austin, G. (1994). Mechanical properties of vacuum-mixed acrylic bone cement. Journal of Applied Biomaterials, 5(4), 307–314. https://doi.org/10.1002/jab.770050405

[40] Krismer, M. (2017). Sports activities after total hip arthroplasty. EFORT Open Reviews, 2(5), 189–194. https://doi.org/10.1302/2058-5241.2.160059

[41] Dalstra M, Huiskes R, Odgaard A, van Erning L. (1993) Mechanical and textural properties of pelvic trabecular bone. J Biomech. 26(4-5):523-35.

[42] Zhang QH, Wang JY, Lupton C, Heaton-Adegbile P, Guo ZX, Liu Q, Tong J. (2010) A subject-specific pelvic bone model and its application to cemented acetabular replacements. J Biomech. 2010 Oct 19; 43(14):2722-7.

[43] Sanjay D, Mondal S, Bhutani R, Ghosh R. (2018). The effect of cement mantle thickness on strain energy density distribution and prediction of bone density changes around cemented acetabular component. Proc Inst Mech Eng H. 2018 Sep;232(9):912-921.

[44] Ghosh R, Gupta S, Dickinson A, Browne M. (2012). Experimental validation of finite element models of intact and implanted composite hemipelvises using digital image correlation. J Biomech Eng. 2012 Aug;134(8); 081003.

[45] Zant, N. P., Heaton-Adegbile, P., Hussell, J. G., & Tong, J. (2008). In vitro fatigue failure of cemented acetabular replacements: a hip simulator study. Journal of biomechanical engineering, 130(2), 021019.

[46] Palermo A, Tuccinardi D, Defeudis G, Watanabe M, D'Onofrio L, Lauria Pantano A, Napoli N, Pozzilli P, Manfrini S, (2016). BMI and BMD: The Potential Interplay between Obesity and Bone Fragility. Int J Environ Res Public Health. 2016 May 28;13(6).

[47] De Groot R, Peters MC, De Haan YM, Dop GJ, Plasschaert AJ. (1987) Failure stress criteria for composite resin. J Dent Res. 1987 Dec;66(12):1748-52.

[48] Dunne, N. (2008). Mechanical Properties of Bone Cements - Orthopaedic Bone Cements. In S. Deb (Ed.), Orthopaedic bone cements (pp. 231-264). Taylor and Francis.

[49] Kühn KD. (2005) Properties of Bone Cement: What is Bone Cement? In: The Well-Cemented Total Hip Arthroplasty - Theory and Practice (Ed. Breusch S and Malchau H). Springer Medizin Verlag. Berlin Heidelberg New York; 52-9.

## Tables

**Table 1** Loading angles and force at hip joint as percentage of body weight for different activities [29].

| Activities | Loading Angle | Load at Hip Joint as Percentage of Body Weight (BW) |
|---|---|---|
| One leg stance | 6.5° | 231% BW |
| Normal walking | 13.1° | 238% BW |
| Ascending stairs | 14.0° | 251% BW |
| Descending stairs | 10.8° | 260% BW |
| Stumbling | 13.1° | 1.25 x (870% BW) |

**Table 2** Mechanical properties.

| Material | Young's Modulus (MPa) | Poisson's Ratio (v) |
|---|---|---|
| Cortical bone | 16,000 | 0.3 |
| Trabecular bone | 155 | 0.3 |
| Acrylic bone cement | 2,000 | 0.3 |
| UHMWPE (Acetabular cup) | 800 | 0.4 |
| Steel (Femoral head) | 207,000 | 0.3 |

**Table 3** Number of tetrahedral and hexahedral elements employed for mesh sensitivity analysis.

| Number of Tetrahedral Elements (C3D10) | | | Hexahedral Elements (C3D20R) | | | | | |
|---|---|---|---|---|---|---|---|---|
| Mesh size | Part | | Part | | | | | |
| | Pelvic bone | Cement mantle | Head 28 mm | Cup 28 mm | Head 32 mm | Cup 32 mm | Head 36 mm | Cup 36 mm |
| Coarse | 105,091 | 11,743 | 160 | 448 | 312 | 448 | 432 | 448 |
| Medium | 162,389 | 15,862 | 704 | 2,336 | 896 | 1,752 | 1,840 | 1,168 |
| Fine | 207,162 | 21,210 | 1,600 | 5,180 | 2,976 | 4,144 | 3,456 | 3,108 |

**Table 4** Dimensions of the acetabular cup and femoral head for the FE models.

| Model | Acetabular cup | | Femoral head |
|---|---|---|---|
| | Outer diameter (mm) | Inner diameter (mm) | Diameter (mm) |
| 1 | 50 | 36.5 | 36 |
| 2 | 50 | 32.5 | 32 |
| 3 | 50 | 28.5 | 28 |

## Figures

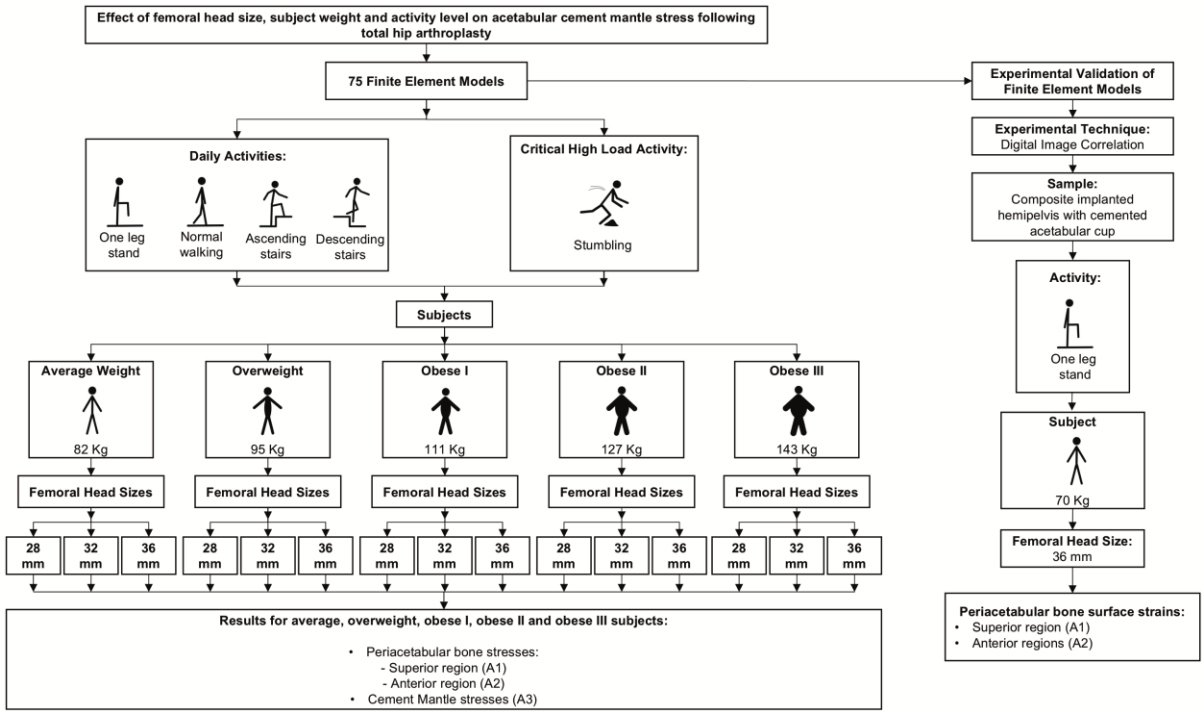


Figure 1 Methodology flowchart.

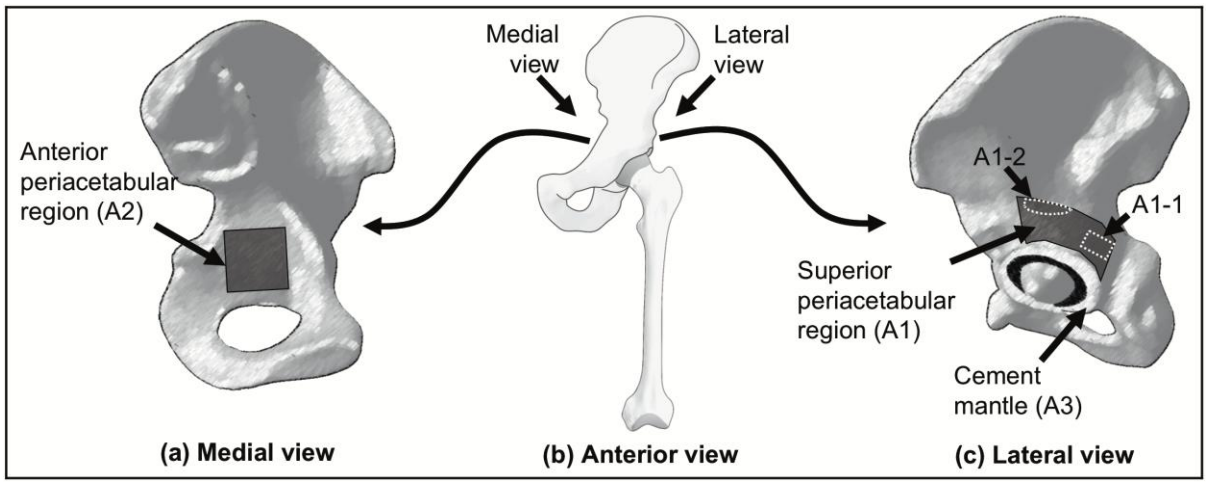


Figure 2 Regions of interest. (a) Region A2 indicated on the medial view of the hemipelvis, (b) schematic of a left hip joint that indicating the medial and lateral views, (c) region A1(A1-1, A1-2) and A3 indicated onthe lateral view of the hemipelvis.

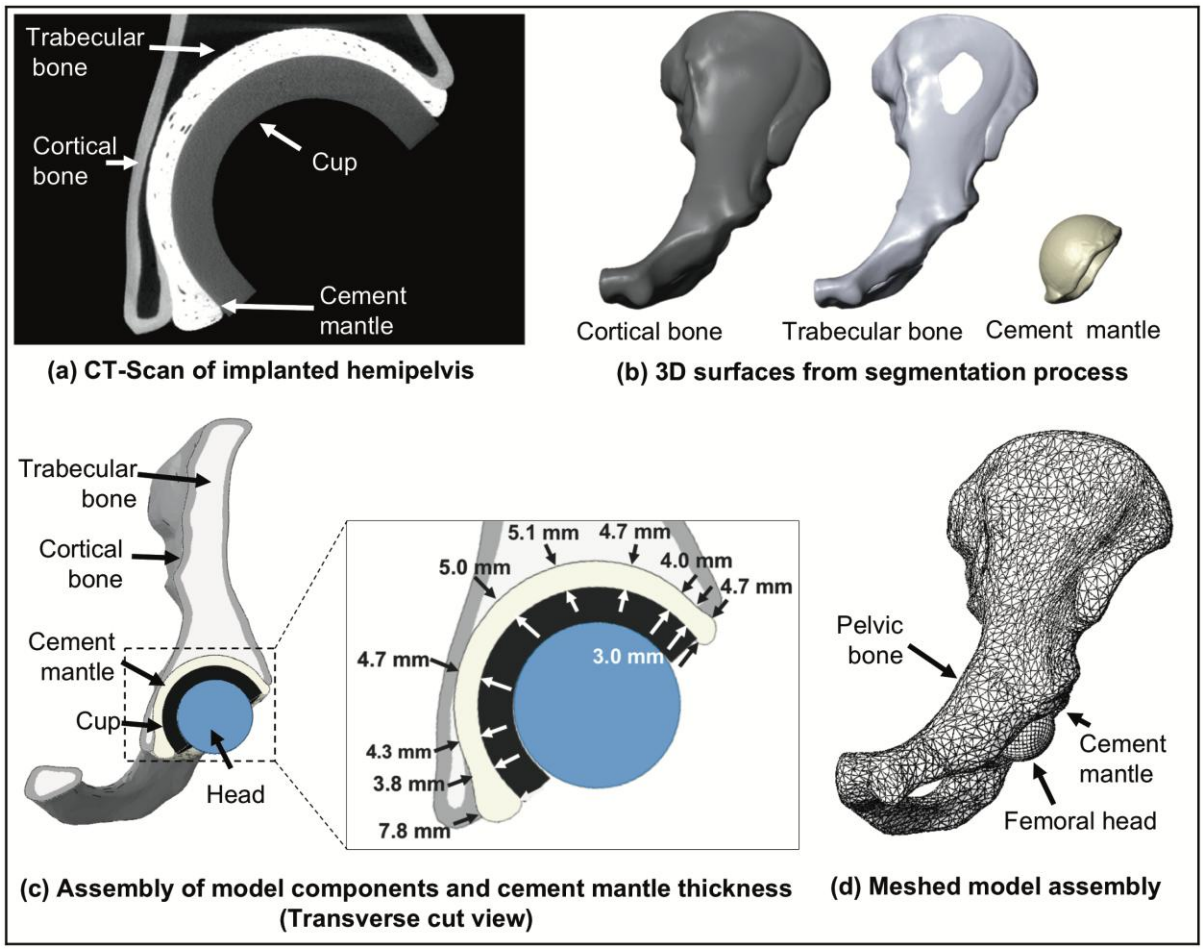


Figure 3 Development of FE model. (a) Segmentation and creation of 3D surfaces from CT-Scan data, (b)measurement of cement mantle thickness, (c) transverse cut view of the assembled model components (Abaqus 6.13), (d) meshed assembly for FE analysis (Abaqus 6.13).

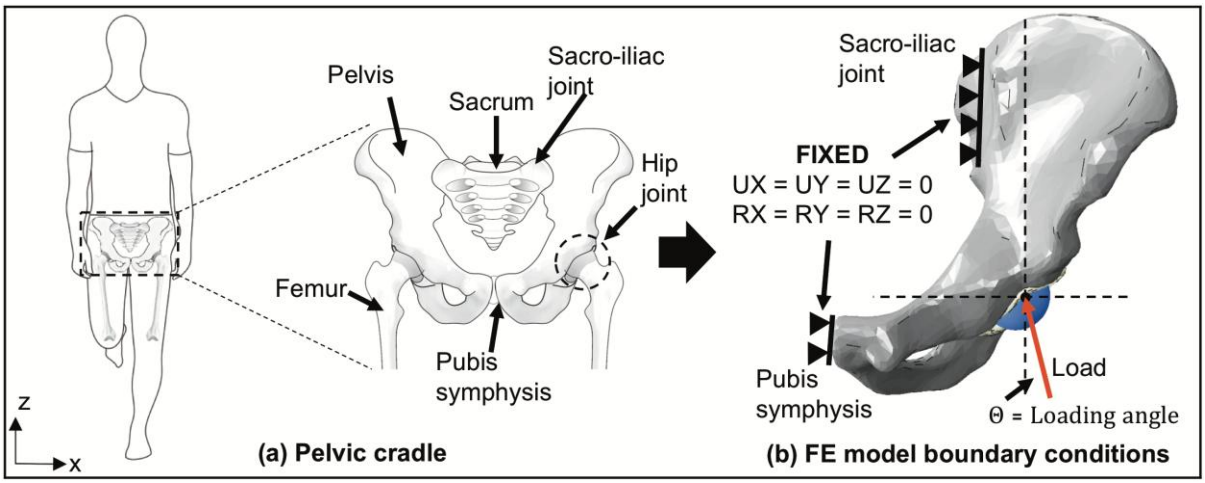


Figure 4 (a) Schematic of complete pelvic cradle showing interaction between sacrum and pelvis at the sacro-iliac joint, and the interaction between pubis symphysis of the two hemipelvis, (b) anterior view of the left hemipelvis showing the boundary conditions of the FE model.

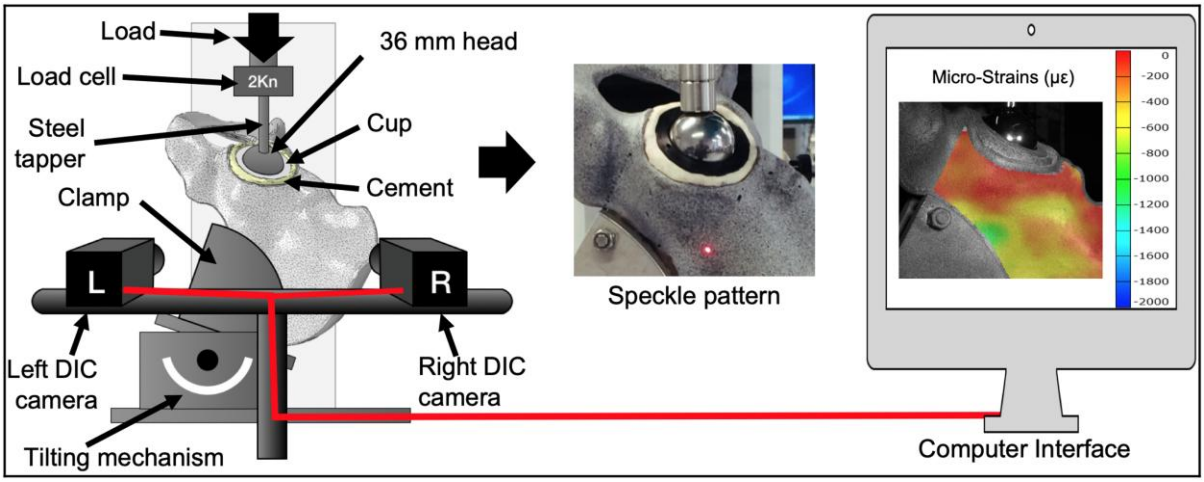


Figure 5 Schematic of experimental setup for the application of the load at the hip joint during one leg stance for the average patient that shows the speckle pattern painted over the surface of the hemipelvis and the DIC cameras used to capture the data.

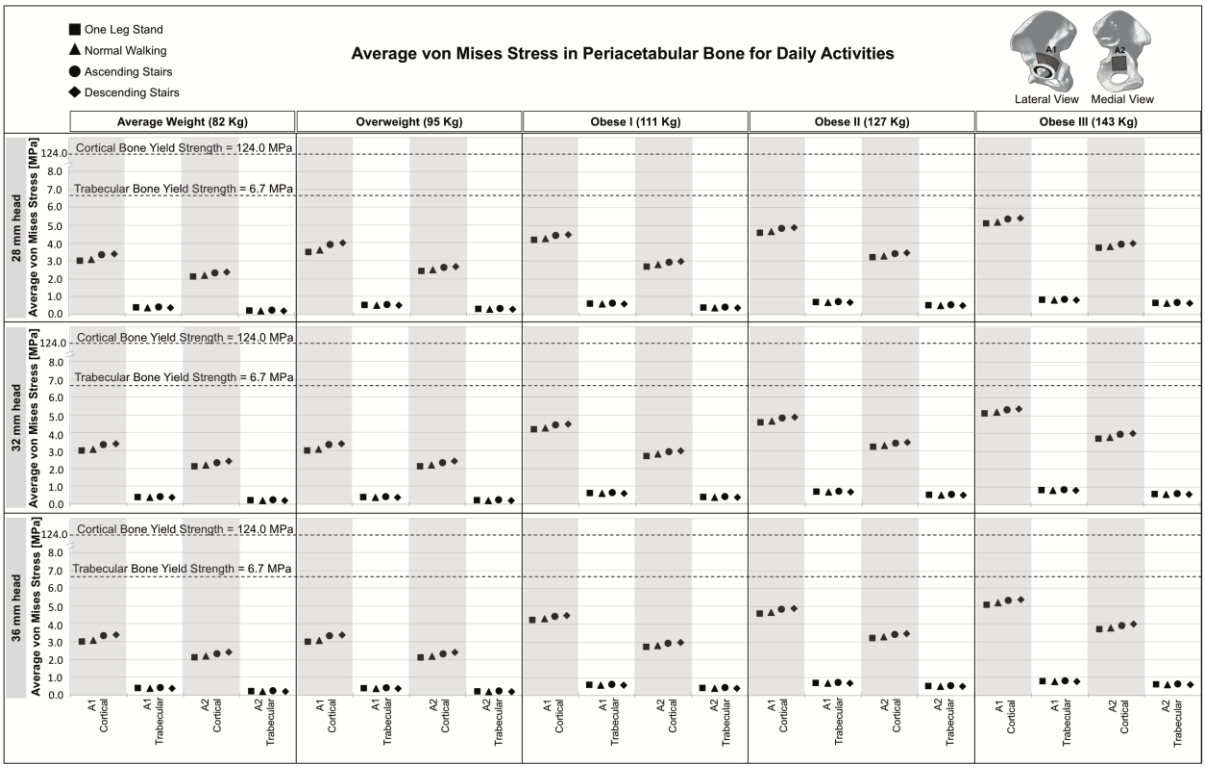


Figure 6 Comparison of cortical and trabecular pelvic bone average von Mises stresses at regions A1 and A2 between the average weight (82 kg), overweight (95 kg), obese I (111 kg), obese II (127 kg) and obese III (143 kg) subjects for femoral head sizes of 28 mm, 32 mm and 36 mm for the daily activities of one leg stand, normal walking, ascending stairs and descending stairs.

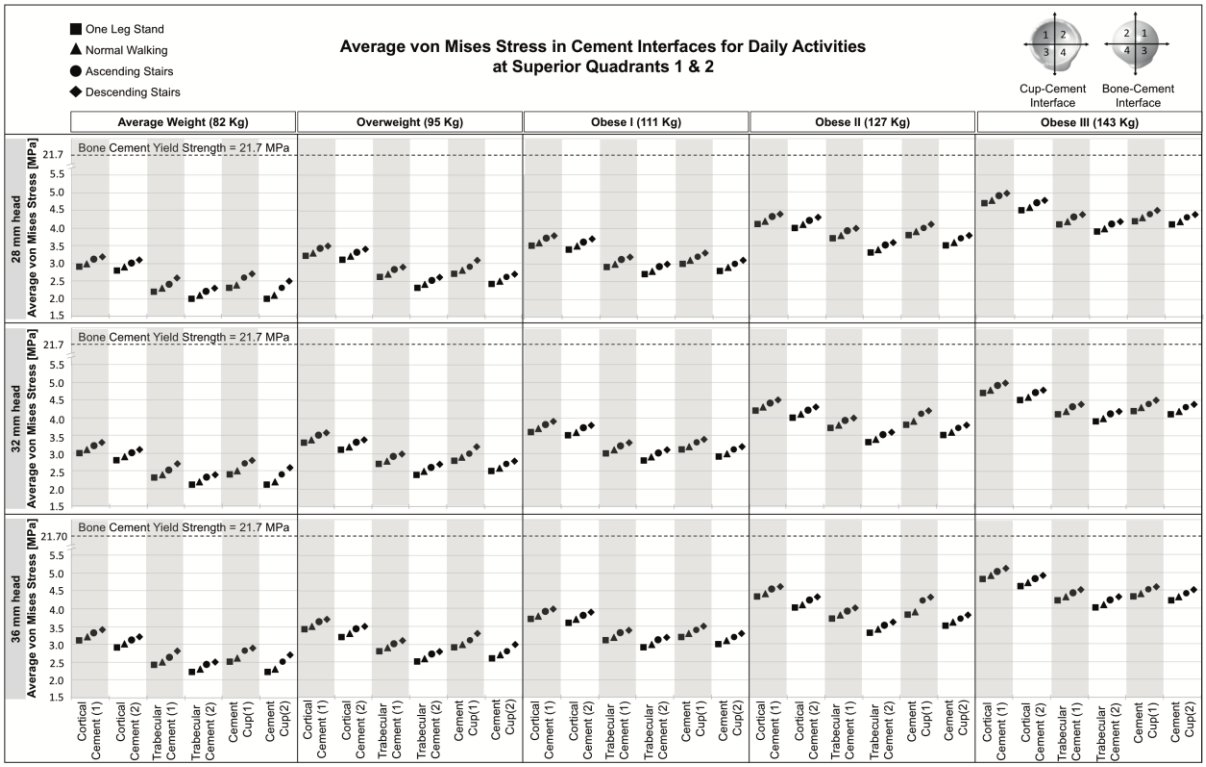


Figure 7 Comparison of average von Mises stresses at the superior quadrants of the bone-cement and cement-cup interfaces between the average weight (82 kg), overweight (95 kg), obese I (111 kg), obese II (127 kg) and obese III (143 kg) subjects for femoral head sizes of 28 mm, 32 mm and 36 mm for the daily activities one leg stand, normal walking, ascending stairs and descending stairs.

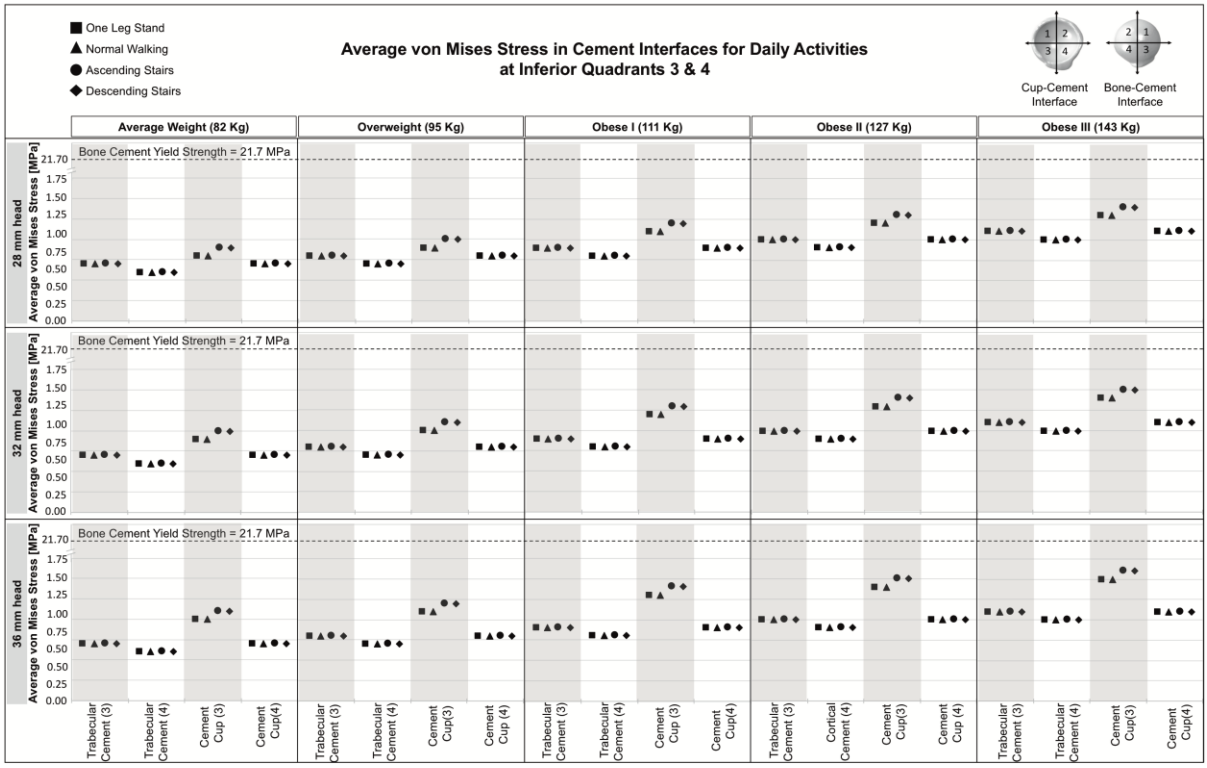


Figure 8 Comparison of average von Mises stresses at the inferior quadrants of the bone-cement and cement-cup interfaces between the average weight (82 kg), overweight (95 kg), obese I (111 kg), obese II (127 kg) and obese III (143 kg) subjects for femoral head sizes of 28 mm, 32 mm and 36 mm for the daily activities one leg stand, normal walking, ascending stairs and descending stairs.

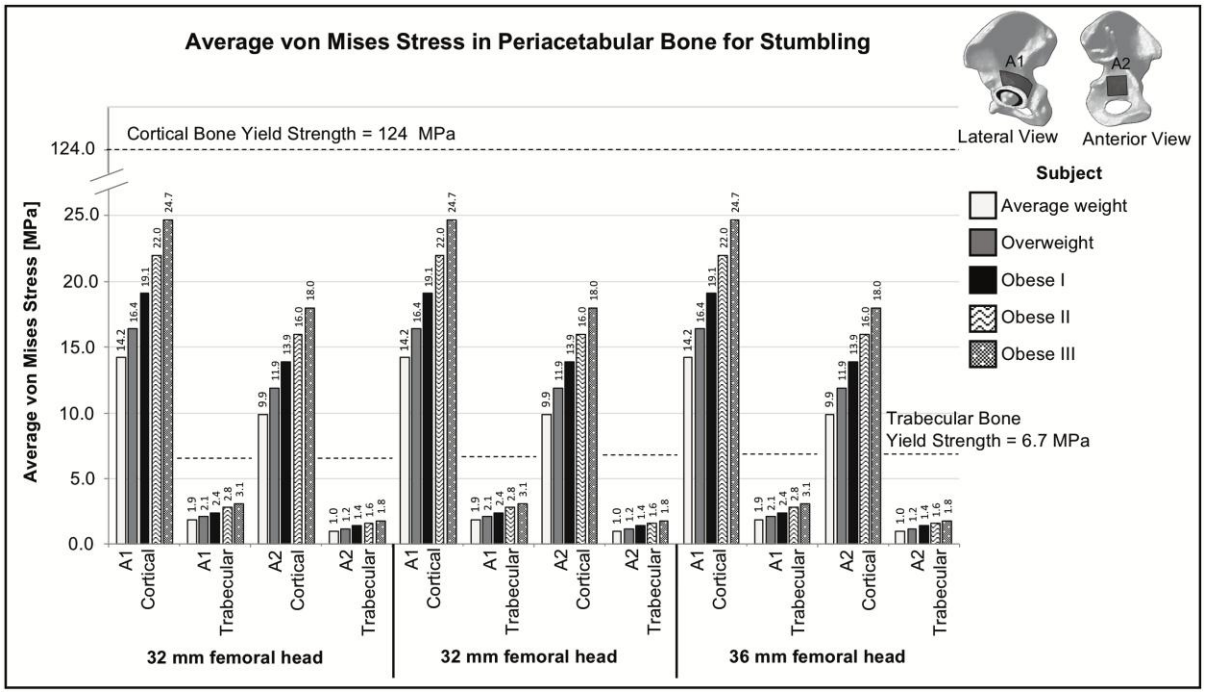


Figure 9 Comparison of cortical and trabecular pelvic bone average von Mises stresses at regions A1 and A2 between the average weight (82 kg), overweight (95 kg), obese I (111 kg), obese II (127 kg) and obese III (143 kg) subjects for femoral head sizes of 28 mm, 32 mm and 36 mm for the critical high load activity stumbling.

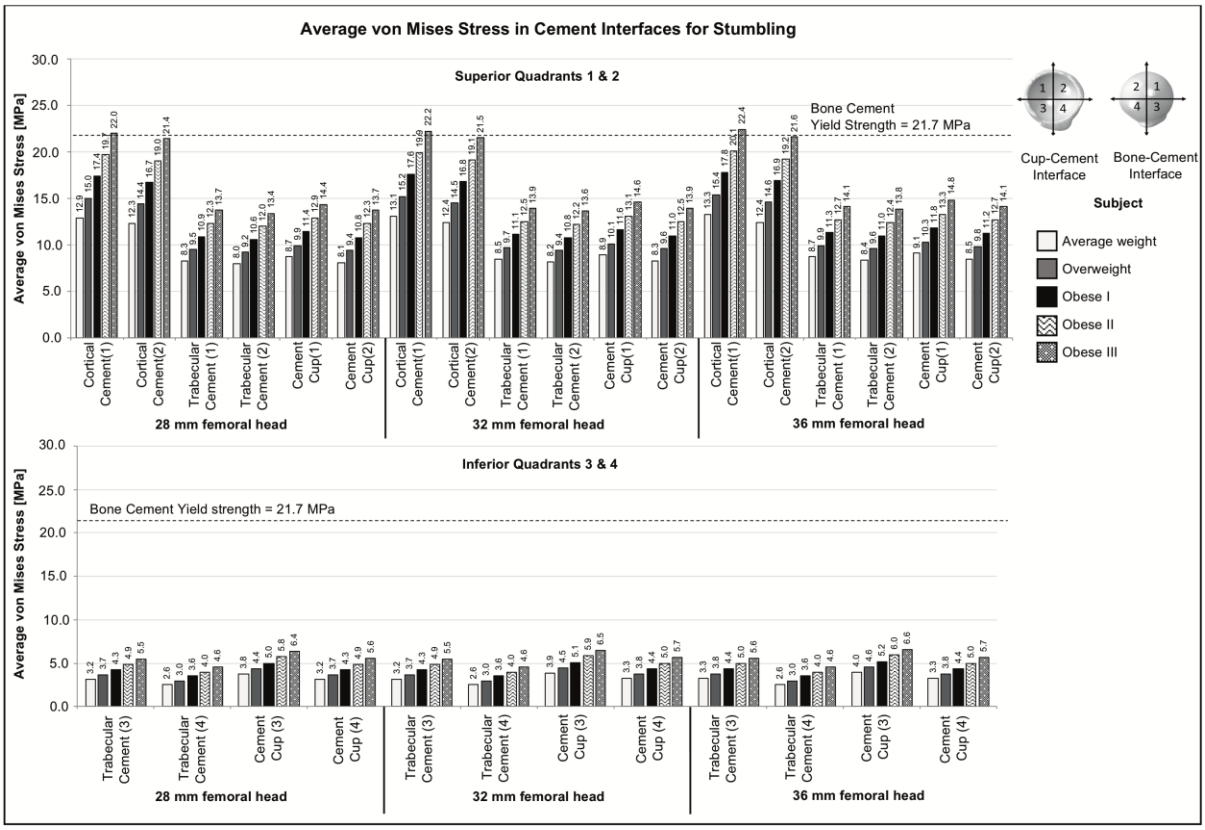


Figure 10 Comparison of average von Mises stresses at the superior and inferior quadrants of the bone cement and cement-cup interfaces between the average weight (82 kg), overweight (95 kg), obese I (111 kg), obese II (127 kg) and obese III (143 kg) subjects for femoral head sizes of 28 mm, 32 mm and 36 mm for the critical high load activity stumbling.